Valence-Bond Charge-Transfer Model for Nonlinear Optical Properties of Charge-Transfer Organic Molecules

Daqi Lu,[†] Guanhua Chen,[†,§] Joseph W. Perry,[‡] and William A. Goddard, III*,[†]

Contribution from the Materials and Molecular Simulation Center, Beckman Institute (139-74), Division of Chemistry and Chemical Engineering (CN 8619), California Institute of Technology, Pasadena, California 91125, and Jet Propulsion Laboratory, Pasadena, California 91109

Received April 26, 1994[⊗]

Abstract: The nonlinear optical properties of charge-transfer organic materials are discussed in the framework of a simple valence-bond charge-transfer model. This model leads to analytic formulas for the absorption frequency, hyperpolarizabilities, and bond length alternation, all of which are described in terms of three parameters, V, t, and Q related to the band gap, bandwidth, and dipole moment of the charge-transfer state. These parameters are derivable from experiment or from theory. The valence-bond charge-transfer model provides a clear physical picture for the dependence of the hyperpolarizabilities on the structure of charge-transfer molecules and leads to good agreement with the trends predicted by the AM1 calculations.

1. Introduction

Nonlinear optical (NLO) materials are playing an increasingly important role for a wide range of applications, including laser technology, telecommunications, data storage, and optical switches.[1–4] Exemplary NLO properties are exhibited by conjugated organic molecules with terminal electron donor and acceptor groups, e.g.

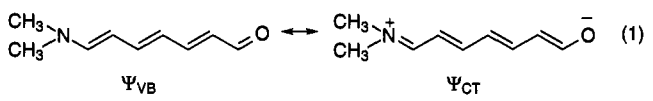

(1)

Such molecules possess a low-energy charge-transfer (CT) state and exhibit large second- and third-order nonlinearities.[5–7] Marder, Perry, and co-workers[7] have studied the NLO properties of a series of such materials and have shown a strong correlation between hyperpolarizabilities and bond length alternation (BLA) in the conjugated bridge. They used solvents of varying polarity to modify the BLA for the conjugated organic molecules and measured the corresponding hyperpolarizabilities. Gorman and Marder[7e] carried out finite-field semiempirical molecular orbital calculations (at the AM1 level) to obtain numerical relationships between hyperpolarizabilities and BLA, with results consistent with experimental trends. However, there is not yet a simple analytical model to explain the relationship between BLA and the various order polarizabilities.

Here we start with the valence-bond charge-transfer model (VB-CT) previously used to describe the hyperpolarizabilities of polyenes[8] and extend it to systems terminated with donor and acceptor units. This VB-CT model is used to describe the polarizability and hyperpolarizabilities of charge-transfer-type molecules. We derive analytic formulas that explain the relation of the polarizability and hyperpolarizabilities to BLA. Because of its basis in classical resonance theory, this VB-CT model provides insight into the factors determining α, β, and γ.

The basic theory is developed in section 2, and predictions of hyperpolarizabilities are given in section 3. Section 4 compares the VB-CT results to quantum chemical calculations (AM1) and shows how to use the theory in interpreting experimental results and predicting properties.

2. Theory

2.1. The VB-CT Model. We consider a molecule of the form 1, where Ψ_{VB} is the normal valence bond configuration (no CT between donor and acceptor). The second state Ψ_{CT} is obtained by moving an electron from donor to acceptor, leading to the alternative VB description of the intervening polyene unit. Taking the energy of Ψ_{VB} as the reference, the Hamiltonian matrix becomes

$$H_0 = \begin{pmatrix} E_{VB} & -t \\ -t & E_{CT} \end{pmatrix} = \begin{pmatrix} 0 & -t \\ -t & V \end{pmatrix} \tag{2}$$

where $-t = \langle \Psi_{VB} | \mathcal{H} | \Psi_{CT} \rangle$ is the many-body CT matrix element (t is positive),

$$V = E_{CT} - E_{VB} \tag{3}$$

and we assume that $\langle \Psi_{VB} | \Psi_{CT} \rangle = 0$. V is determined by the nature of the donor and acceptor groups, by the topology of

[†] California Institute of Technology.
[‡] Jet Propulsion Laboratory.
[§] Current Address: Department of Chemistry, University of Rochester, Rochester, NY 14627.
* To whom correspondence should be addressed.
[⊗] Abstract published in *Advance ACS Abstracts,* October 1, 1994.

(1) Prasad, P. N., Williams, D. J., Eds. *Introduction to Nonlinear Optical Effects in Molecules and Polymers*, Wiley: New York, 1991.
(2) Kuhn, H., Robillard, J., Eds. *Nonlinear Optical Materials*; CRC Press, Inc.: Boca Raton, FL, 1992.
(3) Ashwell, G. J.; Hargreaves, R. C.; Baldwin, C. E.; Bahra, G. S.; Brown, C. R. *Nature* **1992**, *357*, 393.
(4) Stegeman, G. I.; Burke, J. J.; Seaton, C. T. Nonlinear Integrated Optics. In *Optical Engineering: Integrated Optical Components and Circuits*; Huteheson, L. D., Ed.; Marcel Dekker: New York, 1987; Vol. 13.
(5) Dulcic, A.; Flytzanis, C.; Tang, C. L.; Pepin, D.; Fetizon, M.; Hoppiliard, Y. *J. Chem. Phys.* **1981**, *74*, 1559.
(6) Cheng, L.-T.; Tam, W.; Marder, S. R.; Stiegman, A. E.; Rikken, G.; Spangler, C. W. *J. Phys. Chem.* **1991**, *95*, 10643.
(7) (a) Marder, S. R.; Beratan, D. N.; Cheng, L.-T. *Science* **1991**, *252*, 103. (b) Marder, S. R.; Perry, J. W.; Bourhill, G.; Gorman, C. B.; Tiemann, B. G. *Science* **1993**, *261*, 186. (c) Marder, S. R.; Gorman, C. B.; Tiemann, B. G.; Cheng, L.-T. *J. Am. Chem. Soc.* **1993**, *115*, 3006. (d) Marder, S. R.; *et al. J. Am. Chem. Soc.* **1993**, *115*, 2524. (e) Gorman, C. B.; Marder, S. R. *Proc. Natl. Acad. Sci.* **1993**, *90*, 1129.
(8) Lu, D.; Chen, G.; Goddard, W. A., III. The Valence Bond Charge Transfer Exciton Model for Predicting Nonlinear Optical Properties (Hyperpolarizabilities and Saturation Length) of Polymeric Materials. *J. Chem. Phys.* **1994**, *101*, 4920.

0002-7863/94/1516-10679$04.50/0

the conjugated linker (which determines the change in aromaticity), and by the effect of solvent polarity. Solving for the eigenvalues of (2) leads to the energies

$$E_{gr} = {}^1/_2V - {}^1/_2(V^2 + 4t^2)^{1/2} \quad (4)$$

$$E_{ex} = {}^1/_2V + {}^1/_2(V^2 + 4t^2)^{1/2} \quad (5)$$

where gr and ex indicate the ground and excited states. The energy gap is

$$E_g = (V^2 + 4t^2)^{1/2} \quad (6)$$

which can be related to the wavelength for the maximum in the absorption spectrum

$$\lambda_{max} = \frac{hc}{E_g} \quad (7)$$

Denoting the fraction of the charge-transfer configuration in the ground state as f, we write the ground state eigenfunction as

$$\Psi_{gr} = (1 - f)^{1/2}\Psi_{VB} + (f)^{1/2}\Psi_{CT} \quad (8)$$

From (2) and (4) we obtain

$$\Psi_{gr} = \frac{t}{(t^2 + E_{gr}{}^2)^{1/2}}\Psi_{VB} + \frac{E_{gr}}{(t^2 + E_{gr}{}^2)^{1/2}}\Psi_{CT} \quad (9)$$

so that

$$f = \frac{E_{gr}{}^2}{t^2 + E_{gr}{}^2} = \frac{1}{2} - \frac{V}{2(V^2 + 4t^2)^{1/2}} \quad (10a)$$

or

$$f = \frac{\partial E_{gr}}{\partial V} \quad (10b)$$

2.2. Inclusion of the BLA Coordinate. Since Ψ_{CT} and Ψ_{VB} involve alternate resonant descriptions of the intervening polyene unit, the increase of f from 0 to 1 will change each double bond ($R = 1.33$ Å) of the polyene to a single bond ($R = 1.45$ Å) and vice versa. [These distances are based on the experimental average bond lengths of *trans*-1,3,5,7-octatetraene.[9]] Thus the BLA coordinate changes from $q = -0.12$ Å to $q = +0.12$ Å as the CT fraction f goes from 0 to 1, leading to a one-to-one relationship. We will describe the bond length distortion as a vibrational coordinate by associating potentials in (11) and (12) with the VB and CT states. The vibrational contributions to the Hamiltonian 2 are

$$E_{VB} = {}^1/_2k(q - q^0_{VB})^2 \quad (11)$$

$$E_{CT} = V_0 + {}^1/_2k(q - q^0_{CT})^2 \quad (12)$$

where q^0_{VB} and q^0_{CT} are equilibrium positions and V_0 is the *adiabatic* energy difference for these two states. For $f = 0$, the equilibrium BLA coordinate is $q^0_{VB} = -0.12$ Å, and for $f = 1$, it is $q^0_{CT} = +0.12$ Å. Thus V and the ground state energy E_{gr} are replaced by

$$V = V_0 + {}^1/_2k[(q - q^0_{CT})^2 - (q - q^0_{VB})^2] \quad (13)$$

and

$$E_{gr} = {}^1/_2[V_0 + {}^1/_2k(q - q^0_{VB})^2 + {}^1/_2k(q - q^0_{CT})^2] - {}^1/_2(V^2 + 4t^2)^{1/2} \quad (14)$$

The equilibrium coordinate of Ψ_{gr}, q_{opt}, is obtained by solving

$$\frac{dE_{gr}}{dq} = 0 \quad (15)$$

This leads to

$$q_{opt} = \frac{1}{2}(q^0_{VB} + q^0_{CT}) + \frac{1}{2}(q^0_{VB} - q^0_{CT})\frac{V}{(V^2 + 4t^2)^{1/2}} \quad (16a)$$

$$= q^0_{VB} - f(q^0_{VB} - q^0_{CT})$$

$$= -0.12 + 0.24f \quad (16b)$$

This shows that f and q_{opt} are linearly related to each other. We should note that the V in (16a) is the vertical energy difference in (3) for a *particular* value, q, whereas V_0 is the adiabatic energy difference with each surface at its minimum. Equation 13 with $q = q_{opt}$ and (16a) lead to a nonlinear equation which we solve iteratively for q_{opt}.

Figure 1 illustrates the variation of the ground state potential surface and q_{opt} for $V_0 = 1.0$, 0.0, and -1.0 eV using

$$t = 1.1 \text{ eV} \quad (17a)$$

[derived from the experimental data on molecule 1, see discussion in section 4.4] and

$$k = 33.55 \text{ eV/Å}^2 = 773.7 \text{ kcal/(mol Å}^2) = 5.38 \text{ mdyn/cm} \quad (17b)$$

(from UFF[10]) for the force constants in (11) and (12). V_0 is determined by the nature of the donor, the acceptor, the conjugated linker, the solvent, etc. For $V_0 = 1$ eV (Figure 1a), we obtain $q_{opt} = -0.069$ Å. For $V_0 = 0$ (degenerate VB and CT), we obtain $q_{opt} = 0$ (Figure 1b). Further stabilization of CT to $V_0 = -1$ eV (Figure 1c) reverses the BLA to $q_{opt} = +0.069$ Å.

2.3. Application of an Electric Field. For conjugated donor–acceptor systems such as that in (1), the polarizability and hyperpolarizabilities are dominated by the z component (along the chain axis), and we will ignore all other components. Assuming that only Ψ_{CT} contributes to the dipole moment, we write

$$\mu_{CT} = Q|e|R_{DA} \quad (18a)$$

where Q is the net fraction CT for Ψ_{CT}. In an applied external electric field along the z direction, ϵ, as used in measurements of hyperpolarizabilities, the additional (optical) Hamiltonian is

$$H_1 = \begin{pmatrix} 0 & 0 \\ 0 & -\mu_{CT}\epsilon \end{pmatrix} \quad (18b)$$

(9) Baughman, R. H.; Kohler, B. E.; Levy, I. J.; Spangler, C. W. *Synth. Met.* **1985**, *11*, 37.

(10) Rappé, A. K.; Casewit, C. J.; Colwell, K. S.; Goddard, W. A., III; Skiff, W. M. *J. Am. Chem. Soc.* **1992**, *114*, 10024.

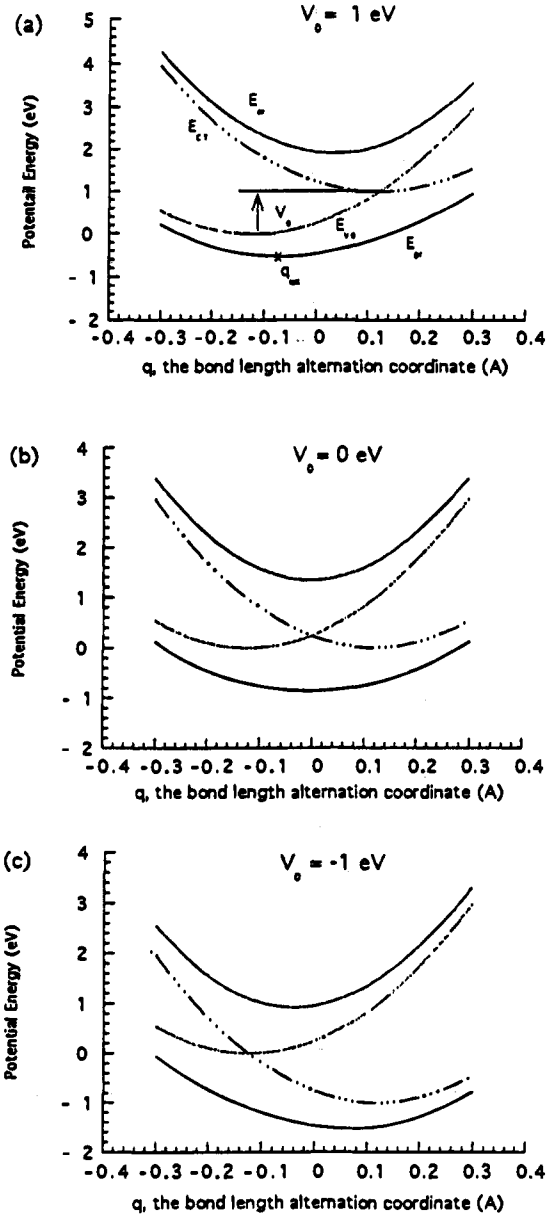

Figure 1. Energies of the ground (E_{gr}) and excited (E_{ex}) states as a function of BLA, q [see eqs 13 and 14]. V_0 is the adiabatic difference between the pure VB and CT states, and q_{opt} is the optimum BLA coordinate. These calculations used k and t from (17). (a) $V_0 = 1$ eV leads to $q_{opt} = -0.069$ Å, (b) $V_0 = 0$ leads to $q_{opt} = 0$, and (c) $V_0 = -1$ eV leads to $q_{opt} = +0.069$ Å.

leading to

$$H = H_0 + H_1 = \begin{pmatrix} E_{VB} & -t \\ -t & E_{CT} - \mu_{CT}\epsilon \end{pmatrix} \tag{19}$$

Thus the relative energy V is replaced by

$$V_\epsilon = V - \mu_{CT}\epsilon \tag{20}$$

Equations 2, 4, and 9 continue to apply for finite applied fields but with V replaced by V_ϵ. In particular, the change in f due to the applied field is

$$\frac{df}{d\epsilon} = \frac{df}{dV_\epsilon}\frac{dV_\epsilon}{d\epsilon} = \frac{2t^2\mu_{CT}}{(V_\epsilon^2 + 4t^2)^{3/2}} = \frac{2t^2\mu_{CT}}{E_g^3} \tag{21}$$

2.4. Polarizabilities. Given the dependence of the ground state energy on the external electric field, the dipole moment of the ground state, P_z, is obtained from

$$P_z(\epsilon) = -\frac{dE_{gr}}{d\epsilon} \tag{22}$$

Assuming that z is the direction along the chain and that ϵ is in this direction, the polarizability and hyperpolarizabilities can then be obtained from

$$\alpha_{zz} = \frac{dP_z}{d\epsilon}|_{\epsilon=0} \tag{23}$$

$$\beta_{zzz} = \frac{1}{2}\frac{d^2P_z}{d\epsilon^2}|_{\epsilon=0} \tag{24}$$

$$\gamma_{zzzz} = \frac{1}{6}\frac{d^3P_z}{d\epsilon^3}|_{\epsilon=0} \tag{25}$$

$$\delta_{zzzzz} = \frac{1}{24}\frac{d^4P_z}{d\epsilon^4}|_{\epsilon=0} \tag{26}$$

Using (9), (14), and (15) we obtain

$$P_z = \mu_{CT}\frac{dE_{gr}}{dV_\epsilon}|_{\epsilon=0} = f\mu_{CT} \tag{27}$$

$$\alpha_{zz} = -\mu_{CT}^2\frac{df}{dV_\epsilon}|_{\epsilon=0} = \frac{2t^2\mu_{CT}^2}{E_g^3} \tag{28}$$

$$\beta_{zzz} = \frac{\mu_{CT}^3}{2}\frac{d^2f}{dV_\epsilon^2}|_{\epsilon=0} = \frac{3t^2\mu_{CT}^3V}{E_g^5} \tag{29}$$

$$\gamma_{zzzz} = -\frac{\mu_{CT}^4}{6}\frac{d^3f}{dV_\epsilon^3}|_{\epsilon=0} = \frac{4t^2\mu_{CT}^4[V^2-t^2]}{E_g^7} \tag{30}$$

$$\delta_{zzzzz} = \frac{\mu_{CT}^5}{24}\frac{d^4f}{dV_\epsilon^4}|_{\epsilon=0} = \frac{5t^2\mu_{CT}^5V[V^2 - 3t^2]}{E_g^9} \tag{31}$$

The following discussions will omit the z subscripts.

3. Predictions of P, α, β, and γ from VB-CT Theory

As f increases from 0 to 1, the VB-CT model leads to a structural evolution in which the polyene double bonds for Ψ_{VB} change to polyene single bonds in Ψ_{CT} and vice versa. Thus each bond decreases or increases by 0.12 Å as f goes from 0 to 1. Since there is a linear relation (eq 16b) between f and q_{opt} (the ground state BLA) and since f determines the polarizability and hyperpolarizabilities, the polarizability and all hyperpolarizabilities are determined by a single BLA parameter, q_{opt}.

This has been anticipated by Marder *et al.*,[7] who pointed out that BLA is a useful parameter in examining the structure–property relationships for NLO materials. They showed that the β and γ values can be tuned through extrema and zero-crossings by varying BLA. In addition, they carried out finite-field AM1 calculations[7e] on molecule 1 and showed the relationships of α, β, and γ to q_{opt}. Their results provide a good test of VB-CT theory.

In order to illustrate the relationships calculated using the VB-CT model, we used (10), (16), and (28)–(31) to calculate

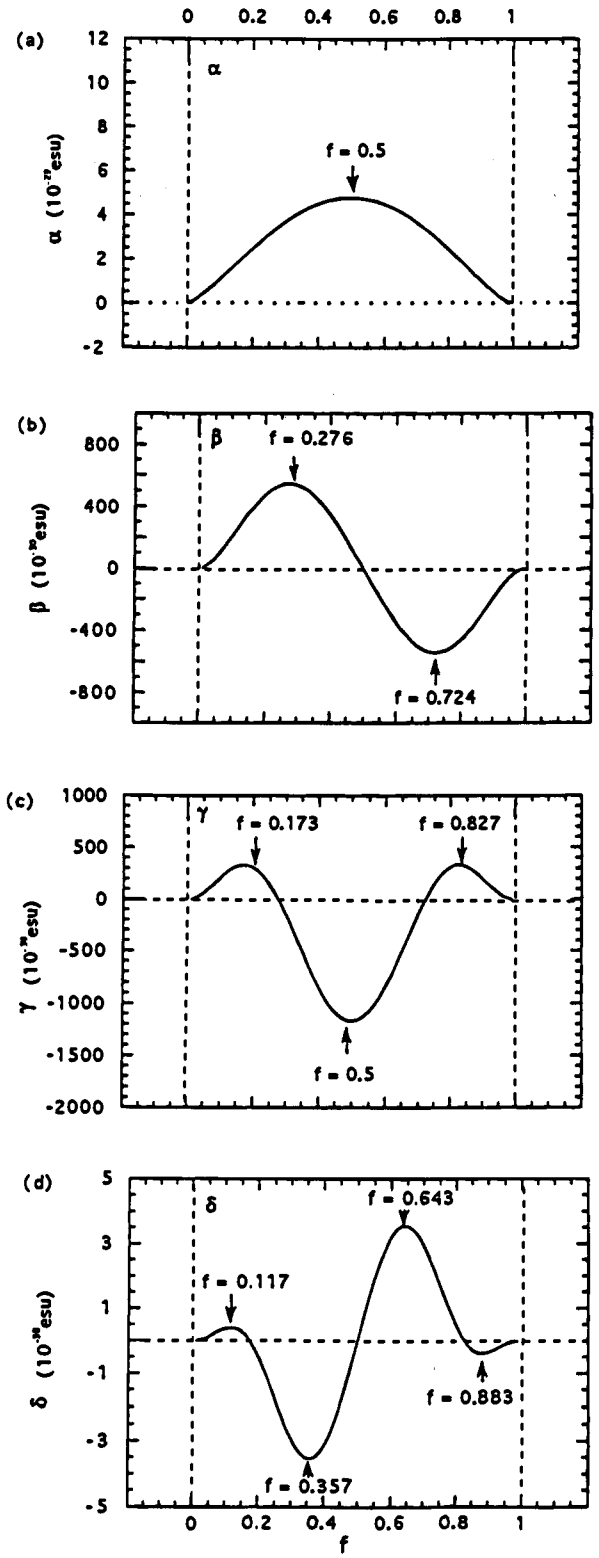

Figure 2. Relation between hyperpolarizability and CT character (f). By (16b), f is directly related to BLA. These calculations used t and k from (17) and $\mu_{CT} = Q|e|R_{DA}$ with $R_{DA} = 9.6$ Å and $Q = 0.69$: (a) polarizability, α; (b) hyperpolarizability, β; (c) second hyperpolarizability, γ; (d) third hyperpolarizability, δ.

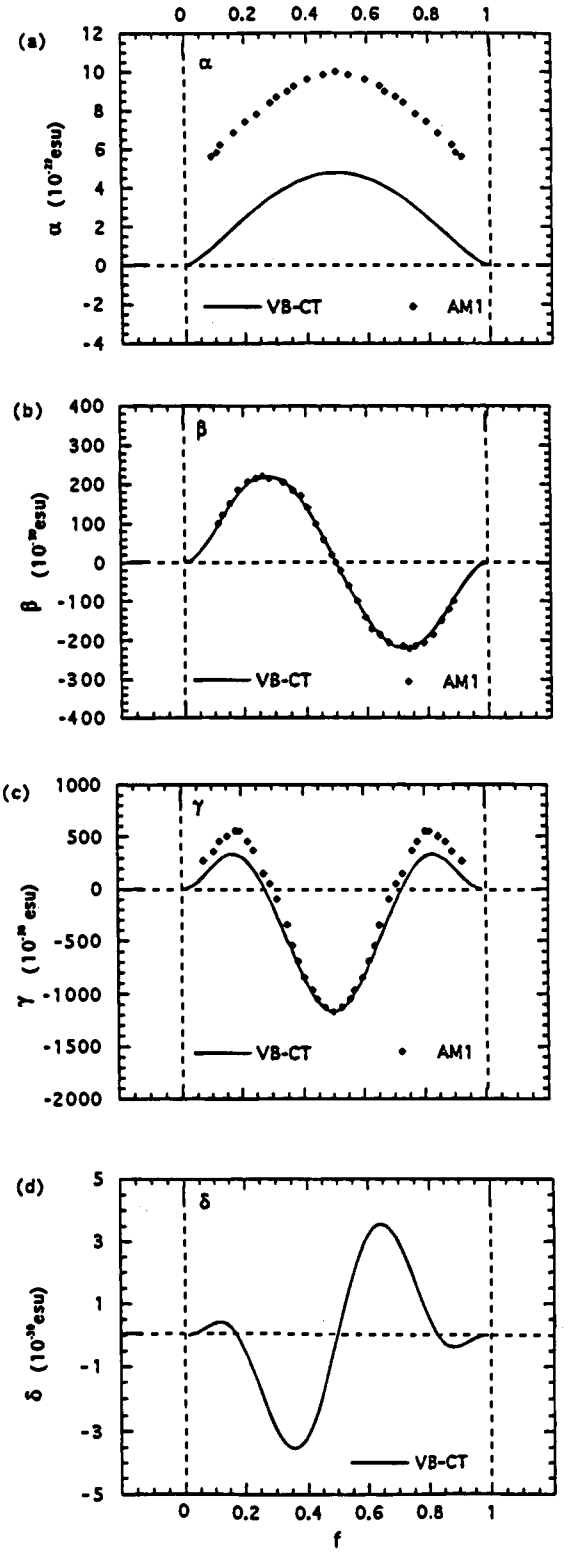

Figure 3. Relation between hyperpolarizability and CT character (f), VB-CT calculation (solid line), and AM1 calculation (squares) (ref 7e). The VB-CT calculation used t and k from (17) and $\mu_{CT} = Q|e|R_{DA}$ with $R_{DA} = 9.6$ Å. The Q values used for α, β, γ, and δ are 0.69, 0.69, 0.51, and 0.69, respectively: (a) polarizability, α; (b) hyperpolarizability, β; (c) second hyperpolarizability, γ; (d) third hyperpolarizability, δ.

f, q_{opt}, α, β, γ, and δ as a function of V, all with the fixed values of t and k from (17). This allowed us to obtain α, β, γ, and δ as functions of q_{opt} (Figure 2).

General observations from these relations are as follows: (i) α has a maximum for $f = 1/2$, which is when all bond lengths in the polyene chain are equal. (ii) β is related to the derivative of α with respect to f, leading to a maximum at $f = 0.276$, a minimum at $f = 0.724$, and a zero value at $f = 1/2$. The maximum and minimum have the same magnitude. (iii) γ is related to the derivative of β with respect to f, leading to the largest magnitude (a minimum) at $f = 1/2$, with secondary maxima (about one-fourth the magnitude) at $f = 0.173$ and $f =$

0.827. $\gamma = 0$ at $f = 0.276$ and $f = 0.724$, where $|\beta|$ is a maximum. (iv) δ is related to the derivative of γ with respect to f, leading to largest magnitudes at $f = 0.357$ (minimum) and $f = 0.643$ (maximum); secondary maxima in the magnitudes occur at $f = 0.117$ (maximum) and $f = 0.883$ (minimum). δ has zeroes at the places where $|\gamma|$ is a maximum ($f = 0.173$, $f = 0.5$, and $f = 0.827$).

These derivative relationships can be understood as follows. From (20), V_ϵ is a linear function of ϵ, leading to

$$\frac{d}{d\epsilon} = \frac{d}{dV_\epsilon}\frac{dV_\epsilon}{d\epsilon} = -\mu_{CT}\frac{d}{dV_\epsilon} \tag{32}$$

The relation between the dipole moment P_z and V_ϵ is plotted in Figure 4a. We assume that the dipole moment of Ψ_{VB} is zero, which corresponds to the limit with $V_\epsilon = +\infty$. The dipole moment P of the CT state is μ_{CT}, which corresponds to the limit with $V_\epsilon = -\infty$. Taking the first, second, and third derivatives of the dipole moment with $-V_\epsilon$ leads to α, β, γ, and δ as shown in Figure 4b–e. The relations between V_ϵ, f, and q_{opt} are expressed in (10) and (16). Changing variables from V_ϵ to q_{opt} leads to

$$\frac{d}{d\epsilon} = -\mu_{CT}\frac{d}{dq_{opt}}\frac{dq_{opt}}{dV_\epsilon} = -0.24\mu_{CT}\frac{df}{dV_\epsilon}\frac{d}{dq_{opt}} \tag{33}$$

in which df/dV_ϵ is negative. The range of V_ϵ, *i.e.* $[-\infty, \infty]$, is mapped onto the range of q_{opt}, $[+0.12, -0.12]$, and the shapes of the curves are similiar.

These results lead to the following observations.

When $V = 0$ (degenerate VB and CT states), we have

$$f = {}^1/_2 \tag{34}$$

$$q_{opt} = 0 \tag{35}$$

and

$$t = E_g/2 \tag{36}$$

At this point, α is a maximum, $\beta = 0$, γ is a minimum (largest magnitude), and $\delta = 0$.

When $|V| = |t|$, we have

$$f = 0.276 \text{ or } 0.724 \tag{37}$$

$$q_{opt} = \pm 0.0538 \text{ Å} \tag{38}$$

and

$$t = \frac{E_g}{(5)^{1/2}} \tag{39}$$

Thus, β takes its maximum (minimum) and $\gamma = 0$.

When $|V| = (3)^{1/2}|t|$, we have

$$f = 0.173 \text{ or } 0.827 \tag{40}$$

$$q_{opt} = \pm 0.0785 \text{ Å} \tag{41}$$

and

$$t = \frac{E_g}{(7)^{1/2}} \tag{42}$$

Thus, $|\gamma|$ is a maximum and $\delta = 0$.

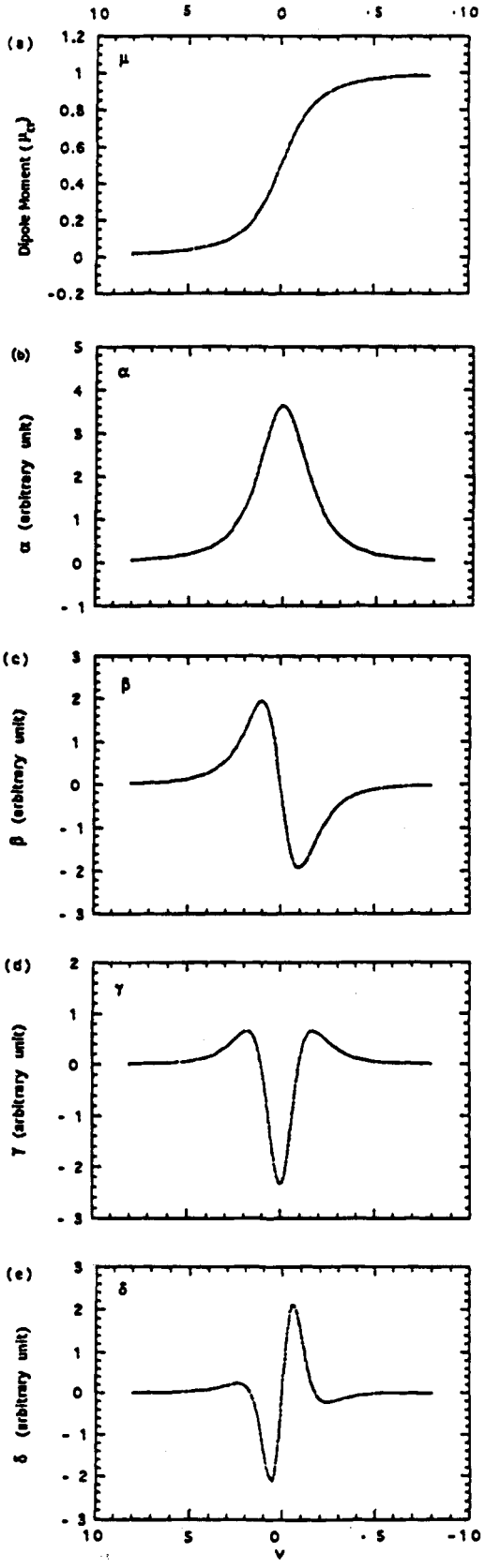

Figure 4. (a) Relation between the dipole moment P_z (in units of μ_{CT}) and V (the VB-CT excitation energy). (b) Polarizability, α, (b) hyperpolarizability, β, (c) second hyperpolarizability, γ, and (d) third hyperpolarizability, δ, obtained from the derivatives of P_z with respect to $-V$ as shown by eqs 28–31.

When $|V| = 0.595|t|$, we have

$$f = 0.357 \text{ or } 0.643 \tag{43}$$

$$q_{opt} = \pm 0.0343 \text{ Å} \quad (44)$$

and

$$t = 0.479E_g \quad (45)$$

Thus, $|\delta|$ takes its largest maxima.

When $|V| = 2.376|t|$, we have

$$f = 0.117 \text{ or } 0.883 \quad (46)$$

$$q_{opt} = \pm 0.0919 \text{ Å} \quad (47)$$

and

$$t = 0.322E_g \quad (48)$$

Thus, $|\delta|$ takes it second largest maxima.

The shapes of the polarizability and hyperpolarizability curves are relatively insensitive to the value t. Thus, the salient factor for polarizability and hyperpolarizabilities is the BLA.

4. Discussion

4.1. Comparison with AM1 Calculations. The VB-CT results are compared with AM1 calculations[7e] (squares) in Figure 3. [The AM1 calculations led to a limiting BLA of 0.108 Å, whereas the experimental value for octatetraene is 0.12 Å; consequently, for AM1, $q_{opt} = -0.108$ for $f = 0$ and $q_{opt} = +0.108$ for $f = 1$.] In Figure 2, we used Q values of 0.69, 0.51, 0.69, and 0.69 to scale the curves for α, β, γ, and δ, respectively.

The AM1 results for β and γ agree quite well with VB-CT theory. VB-CT has α going to zero as $f \rightarrow 0$ or 1, whereas the AM1 calculations lead to about one-half the maximum. This is probably because the current VB-CT calculations ignore the polarizability for a fixed VB or CT structure (it could have been included as an additive correction).

4.2. Comparison with Two-Level Models. Two-level models have been used widely to understand the NLO properties of materials.[11] In the absence of an external electric field, the system is described in terms of two eigenvectors corresponding to the ground and excited states. Upon applying an electric field ϵ, the additional Hamiltonian term $-\epsilon\cdot\mu$ is treated as a perturbation, where μ is the dipole moment matrix

$$\mu = \begin{pmatrix} \mu_{gg} & \mu_{ge} \\ \mu_{ge} & \mu_{ee} \end{pmatrix} \quad (49)$$

This leads, for example, to a first hyperpolarizability β of the form

$$\beta \sim (\mu_{ee} - \mu_{gg})\frac{\mu_{ge}^2}{E_{ge}^2} \quad (50)$$

where E_{ge} is the energy gap. This expression results from the change in ground state energy due to field but does not account explicitly for the change in structure due to the modified equilibrium position of the ground state potential. Thus, it does not provide a form for the higher polarizabilities and does not provide an explicit picture for the structure–property relationships illustrated above.

The VB-CT model differs from such two-level models because the NLO properties are treated as due to the dependence of the dipole moment on the "field" (the VB-CT adiabatic energy difference, V), which in turn depends on the mixing of VB and CT and the resultant change in structure. This VB-CT picture allows the calculation of changes in structure and of the structure–NLO property relationships with only a few chemically meaningful parameters. This leads to a direct relationship between α, β, γ, and δ as the structure varies between a neutral polyene-like structure and a zwitterionic structure.

4.3. Additional Excited States. The VB-CT model assumes that all other excited states are much higher than the VB and CT states. In particular, the resonant states (eq 51) involving

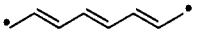
(51)

the bridge or linker must be much higher. For octatetraene 52, the absorption maximum is about 4 eV, indicating that the resonant state of the linker in (1) is about 4 eV above the VB state.[12] Since the donor–acceptor molecules considered here

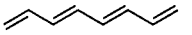
(52)

have the CT state about 1–2 eV above the VB state, neglect of the resonant state should be a good approximation. When the energy of the resonant state is close to those of VB and CT, the contributions from the linker resonant state must be included. This complicates the theory so that the results are no longer analytic. However, combining the current VB-CT theory for donor–acceptor molecules with the VB-CT-E theory[8] for polymer linkers is straightforward and under development.[13]

4.4. Applications to Various Molecules. To illustrate the application of the VB-CT model, we will consider the nonlinear polarizabilities of several donor–acceptor molecules linked by a conjugated octatetraene chain. As described in section 3, t can be explicitly related to λ_{max} for certain structural limits. Given t, one can use the expressions and the relationships given above to identify molecules that would have properties near the peak values or zero-crossings of the polarizabilities.

For the case of the four double bond cyanine (53), λ_{max} was

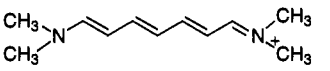
(53)

measured to be 516 nm in CH_3CN solvent, with $\gamma = -370 \times 10^{-36}$ esu.[14] By symmetry this system has $f = 0.5$, leading to $t = E_g/2$, and hence $t = 1.18$ eV. From (37) we predict that a molecule of the same length and linker type but with $E_g = (5)^{1/2}t$ would lead to $\gamma = 0$ and a positive maximum in β. Using $t = 1.18$ eV, this would occur at $\lambda = 467$ nm. In fact, in the solvents C_6H_6 and dioxane, (54) has $\lambda_{max} = 472$ nm and $\lambda_{max} = 468$

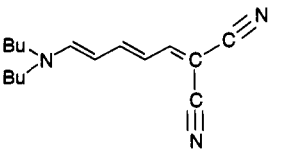
(54)

nm, respectively, and γ changes from 15×10^{-36} to -25×10^{-36} esu with a positive peak observed for $\mu\beta$![15-16]

(11) Beratan, D. Electronic Hyperpolarizability and Chemical Structure. In *Materials for Nonlinear Optics: Chemical Perspectives*; Marder, S. R., Sohn, J. E., Stucky, G. D., Eds.; American Chemical Society: Washington DC, 1991; Vol. 455, pp 89–102. Oudar, J. L. *J. Chem. Phys.* **1977**, *67*, 446.

(12) Granvill, M. F.; Holtom, G. R.; Kohler, B. E. *J. Chem. Phys.* **1980**, *72*, 4671.

(13) Lu, D.; Chen, G.; Goddard, W. A., III. Work in progress.

(14) Bourhill, G.; Tiemann, B. G.; Perry, J. W.; Marder, S. R. Effect of Aromaticity on the Second Hyperpolarizability of Conjugated Donor-Acceptor Molecules. *Nonlinear Opt.*, in press.

(15) Bourhill, G.; Cheng, L.-T.; Gorman, C. B.; Lee, G.; Marder, S. R.; Perry, J. W.; Perry, M. J.; Tiemann, B. T. *Proc. SPIE–Int. Soc. Opt. Eng.* **1994**, 2143.

From (40), we expect γ to have a positive maximum when $E_g = (7)^{1/2}t$ or $\lambda_{max} = 394$ nm. Experimentally, (55) is

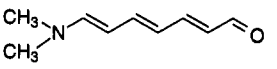

(55)

observed[15] to have a positive peak in γ for solvent CH_3CN, as well as a $\lambda_{max} = 418$ nm, close to the prediction from the VB-CT model. Thus, (55) has $t = E_g/(7)^{1/2} = 1.10$ eV.

Thus, spectroscopic measurements of λ_{max}, together with selected NLO data, can be utilized to predict structures and solvents needed to attain desired structure–NLO property relationships. Elsewhere[17] we will consider a more complete description of solvent effects.

5. Summary

We presented the VB-CT model to provide a simple means for predicting NLO properties of CT-type organic molecules and for explaining in simple analytic terms the relationship between these properties and structure. The absorption frequency, hyperpolarizabilities, and BLA are expressed in terms of analytic formulas with a total of four independent parameters, V, t, Q, and k. Here k is a force constant appropriate for the BLA coordinate of polyene linkers and should be similar for all such materials (it might depend on polyene length, and we used a k based on the universal force field).[10] Q is the ratio of the actual dipole moment of the excited CT state to that expected for perfect CT. This value will depend mainly on polyene length but will be close to the values used here ($Q = 0.5-0.7$). V and t are related to band gap (λ_{max}) and to bandwidth. The value of t is mainly determined by the length of the polyene spacer as well as the coupling of the donor and acceptor to the spacer. Thus, the variable most accessible to design is V, which can be modified by changing the strength of the donor or the acceptor, the bridge topology, or the solvent polarity.[18] The polarizabilities for various materials can be determined by estimating V on the basis of band gap measurements.

We have shown how α, β, γ, and δ are related by derivatives of the CT fraction f. This indicates how the design of molecules with an appropriate value of f can lead to optimization of particular properties, while minimizing the others.

Acknowledgment. We wish to thank Dr. Seth Marder for stimulation and helpful discussion. The research was funded by the NSF (CHE 91-100289). The facilities of the MSC/BI are also supported by grants from DOE-AICD, NSF-ACR, BP America, Allied-Signal Corp., Asahi Chemical, Asahi Glass, Chevron Petroleum Technology Co., BF Goodrich, Teijan Ltd., Vestar, Hughes Research Laboratories, and Beckman Institute. Some calculations were carried out on the JPL Cray and at the Pittsburgh NSF Supercomputing Center. Part of this work was performed at the Jet Propulsion Laboratory, California Institute of Technology, and this portion was supported by the Ballistic Missile Defense Organization/Innovative Science and Technology Office through an agreement with NASA.

(16) Marder, S.; Gorman, C. B.; Meyers, F.; Perry, J. W.; Bourhill, G.; Brédas, J.; Pierce, B. M. A Unified Description of Linear and Nonlinear Polarization in Organic Polymethine Dyes. *Science* **1994**, *265*, 632.

(17) Chen, G.; Lu, D.; Goddard, W. A., III. The Valence-Bond Charge-Transfer Solvation Model (VB-CT-S) for Nonlinear Optical Properties of Organic Molecules in Polar Solvents. *J. Chem. Phys.* **1994**, *101*, 5860.